Highlighting work on electrochemiluminescence (ECL) thin films presented by Prof. Dongpeng Yan and co-workers at Beijing University of Chemical Technology and Beijing Normal University, Beijing, China.

A 2D quantum dot-based electrochemiluminescence film sensor towards reversible temperature-sensitive response and nitrite detection

Orderly self-assembled CdTe quantum dot thin films with highly enhanced anodic electrochemiluminescence (ECL) were developed. The anodic ECL signal of the films is highly sensitive to the change in temperature, and can also serve as a nitrite sensor.

As featured in:

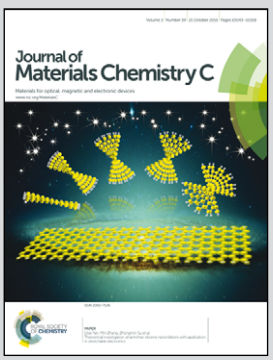

See Dongpeng Yan *et al.*, *J. Mater. Chem. C*, 2015, **3**, 10099.

ROYAL SOCIETY OF CHEMISTRY

www.rsc.org/MaterialsC

Registered charity number: 207890

Journal of Materials Chemistry C

PAPER

View Article Online
View Journal | View Issue

Cite this: J. Mater. Chem. C, 2015, 3, 10099

A 2D quantum dot-based electrochemiluminescence film sensor towards reversible temperature-sensitive response and nitrite detection†

Yuqiong Zhou,[a] Dongpeng Yan*[ab] and Min Wei[a]

Received 3rd July 2015,
Accepted 20th August 2015

DOI: 10.1039/c5tc02002f

www.rsc.org/MaterialsC

The development of a high-efficiency electrochemiluminescence (ECL) system plays an important role in the fields of chemical sensors and environmental detection. Herein, a CdTe quantum dot (QD)-based thin film (TF) with highly enhanced anodic ECL intensity was developed by combining CdTe with Co–Al-layered double hydroxide (LDH) nanoparticles. Through a layer-by-layer (LBL) process, the as-fabricated CdTe/LDH ECL sensor exhibited a high emissive intensity, good sensitivity and long-term stability, and was further used as a bi-functional sensor for temperature response and nitrite detection. The growth of the CdTe/LDH film was firstly monitored by UV-vis absorption and fluorescence spectra. SEM images showed that the film surface presents a continuous and uniform morphology. A temperature-triggered ECL intensity switch for CdTe/LDH was obtained between 20 and 80 °C with a rather high response sensitivity (−1.92% per °C) and good reversibility. Besides, ECL detection of nitrite anions was performed, and a linear response was obtained in the range of 1×10^{-6} to 1×10^{-2} M with a detection limit of 0.719 μM. Moreover, the CdTe/LDH film for nitrite detection showed a fast, selective and reversible ECL response. Therefore, it is expected that the LBL film in this work can provide an effective way to apply QDs as an anodic ECL system in highly sensitive temperature and nitrite sensors.

Introduction

Electrogenerated chemiluminescence (ECL) is the production of light from a high-energy electron-transfer reaction between electro-generated species.[1] In a sense, ECL is a form of CL, and both ECL and CL involve the production of light by species that can undergo highly energetic electron-transfer reactions.[2] Moreover, ECL is also an electrochemical analytical technique. Therefore, by the combination of both chemiluminescence (CL) and electrochemistry, ECL not only holds the sensitivity and wide dynamic range inherent to conventional CL, but also exhibits several advantages of typical electrochemical methods (such as simplicity, stability and facility). Since the pioneering work of Bard *et al.*, who explored the ECL properties of silicon semiconductor nanocrystals (also known as quantum dots (QDs)) in 2002, the preparation and application of various QDs with ECL activity have received growing interest.[3] In the presence of co-reactants (such as $K_2S_2O_8$ and H_2O_2), most of the QDs showed cathodic ECL and can be used to develop ECL sensors based on emission quenching or enhancement *via* charge and/or energy transfer.[4–9] However, the anodic ECL intensity of QDs is still much lower than that of conventional luminescent reagents, and QDs in the ECL process usually involve a high excited potential, resulting in an unstable ECL intensity. Although great efforts have been made for the improvement of the anodic ECL performance of QDs, the emission is still not strong enough compared to that of cathodic ECL.[10,11] Therefore, the development of new QD-based ECL systems with strong and stable anodic ECL is highly desirable.

Among the semiconductor QDs, CdTe has been paid much attention in both photoluminescence (PL) and CL studies, because of its unique luminescence properties and relatively low cost. Additionally, several ECL sensors have been developed with CdTe QDs as ECL emitters. However, there are still two significant barriers for developing CdTe QD-based anodic ECL sensors. One is the limited ECL efficiency of CdTe QDs, *e.g.* the ECL intensity of QDs is not comparable with those of conventional ECL reagents,[12] and thus various signal amplification units[13,14] (including nanoparticles,[15] enzymes,[16] and multiple DNA cycle signals[17]) have to be utilized for improving the sensitivity. Moreover, the limited monodispersity can usually result in completely passivated QDs and a broad ECL spectrum. Therefore, how to fabricate new types of CdTe QD-based anodic ECL sensors

[a] State Key Laboratory of Chemical Resource Engineering, Beijing University of Chemical Technology, Beijing 100029, P. R. China.
E-mail: yandongpeng001@163.com, yandp@mail.buct.edu.cn;
Fax: +86-10-64425385; Tel: +86-10-64412131
[b] Key Laboratory of Theoretical and Computational Photochemistry, Ministry of Education, College of Chemistry, Beijing Normal University, Beijing 100875, China

† Electronic supplementary information (ESI) available: details of the CoAl-LDH hexagonal nanoplatelets, UV/vis and luminescence spectra of the pristine CdTe QD solution, HTEM image of the CdTe QDs, Nyquist plots of EIS for (CoAl-LDH/CdTe QDs)$_n$/ITO, ECL intensities of CdTe QD solutions with different concentrations. See DOI: 10.1039/c5tc02002f

with high sensitivity, stability and reproducibility remains a major goal.

Layered double hydroxides (LDHs) are a class of two-dimensional (2D) clay materials, which can be described by the general formula $[M^{II}_{1-x}M^{III}_{x}(OH)_2]^{z+}A_{z/n}{}^{n-}\cdot yH_2O$ (M^{II} and M^{III} are divalent and trivalent metals, respectively; A^{n-} is the anion).[18] As one type of important inorganic material, LDHs represent a large versatility and high stability, and LDH nanoparticles have been widely used in the immobilization of photoactive and electroactive species in order to fabricate functional thin films (TFs) towards sensor and detection applications.[19–22] In several previous works, the assembly of QDs with LDHs gave rise to tunable photoluminescence (PL) and electroluminescence (EL) applications.[23,24] However, how to combine the advantages of the two components to obtain a high-efficiency ECL sensor remains a challenge. Herein, we present a TF system based on the layer-by-layer (LBL) assembly of mercaptosuccinic acid-modified CdTe QDs and positively-charged CoAl-LDH nanoparticles. The selection of CoAl-LDH is based on the fact that it holds favorable conductivity. On the whole, the incorporation of CdTe QDs within a CoAl-LDH host matrix may possess the following advantages: (1) the electroactive Co-based LDH units can largely accelerate the electron transfer and electrode reaction during the ECL process, (2) the LDH nanoparticles can provide a confined and stable microenvironment for the immobilization and homogeneous distribution of CdTe QDs based on host–guest interactions, which can largely reduce the aggregation-induced ECL quenching, and (3) the solid matrix would enhance the stability of CdTe QDs and suppress their leaching, which meets the prerequisite for the fabrication of solid-state ECL sensors. It was observed that the ECL signal of the CdTe/LDH TFs was highly amplified compared with those of the pristine CdTe solution and CdTe/polymer thin film. Moreover, the as-prepared ECL sensor exhibited good repeatability and long-term stability. In particular, the CdTe/LDH presents a reversible temperature ECL response and high sensitivity for nitrite detection. To the best of our knowledge, this work is the first report on a hybrid QD film as a temperature-dependent anodic ECL sensor. Therefore, this strategy provides an effective way to apply QDs as anodic ECL emitters in a temperature-sensitive response and selective detection of nitrite.

Experimental

Materials

Analytical grade chemicals including $Co(NO_3)_2\cdot 6H_2O$, $Al(NO_3)_3\cdot 9H_2O$, NaOH, $NaBH_4$, K_2HPO_4, $NaNO_3$, and $CdCl_2\cdot 2.5H_2O$ were purchased from J&K Chemical Co. Ltd, and were used without further purification. Sodium tellurate, mercaptosuccinic acid and poly(dimethyldiallylammonium chloride) (PDDA) were purchased from Sigma-Aldrich Co. Ltd. Deionized and decarbonated water was used in the preparation processes.

Synthesis of QDs

The mercaptosuccinic acid-stabilized CdTe nanoparticles were synthesized according to the literature[25] with some modification. Briefly, 100 mL of 0.02 M $CdCl_2$ was mixed with mercaptosuccinic acid (0.3 mmol), and the pH of the mixture was adjusted to 10.5 using 1 M NaOH. The resulting clear solution was bubbled with highly pure N_2 for 30 min. Then, $NaBH_4$ (0.1 g) and $NaTeO_3$ (0.0222 g) were slowly injected into the vigorously stirred and oxygen-free solution to obtain a yellow-brown solution of mercaptosuccinic acid-modified CdTe. The molar ratio of Cd^{2+}/MSA (mercaptosuccinic acid)/$TeO_3{}^{-}$ was 2 : 3 : 1. The obtained QD solution was heated to 90 °C and refluxed for 6 hours to produce CdTe QDs with red-light emission.

Synthesis of CoAl-LDH nanoparticles

A colloidal LDH suspension was prepared according to the separate nucleation and aging steps (SNAS) reported previously.[26] Typically, 100 mL of solution A (0.2 M $Co(NO_3)_2\cdot 6H_2O$ and 0.1 M $Al(NO_3)_3\cdot 9H_2O$) and 400 mL of solution B (0.15 M NaOH) were simultaneously added to a colloid mill with a rotor speed of 3000 rpm and mixed for 1 min. The resulting LDH slurry was obtained *via* centrifugation, washed with water, and then dispersed in 400 mL of deionized water. The aqueous suspension was transferred into a stainless steel autoclave with a Teflon lining. After hydrothermal treatment at 110 °C for 24 h, a stable homogeneous CoAl-LDH suspension with a narrow size distribution can be obtained.

Fabrication of the LDH/CdTe QD multilayer film-modified electrode

ITO glass substrates (1 cm × 3 cm, 10 Ω per square) were cleaned in an ultrasonic bath using the following reagents in sequence: acetone, ethanol and water for 10 min each. After the cleaning procedure, the surfaces of substrates were hydrophilic and negatively charged. The substrates were stored in deionized water before use. Quartz glass (1 cm × 3 cm) substrates were cleaned by immersing in a fresh piranha solution (H_2SO_4 : H_2O_2 (30%) = 3 : 1, v/v) (**Warning**: piranha solution is highly corrosive and must be treated with extreme care) for 40 min, followed by rinsing in deionized water and drying at 60 °C. The $(LDH/CdTe\ QDs)_n$ multilayer films were fabricated by applying the LBL assembly technique: the substrate was alternately dipped into a colloidal LDH nanoparticle suspension (1.0 mg mL^{-1}) and a CdTe QD solution (1.0 mg mL^{-1}) for 10 min each time. The resulting films were dried under a nitrogen gas flow for 2 min at 25 °C. Subsequently, the series of these two deposition operations was repeated for n times to obtain a multilayer film of $(LDH/CdTe\ QDs)_n$ (Fig. 1).

Characterization techniques

UV-vis spectra were collected on a Shimadzu U-3000 spectrophotometer. Zeta potentials were determined by a Malvern

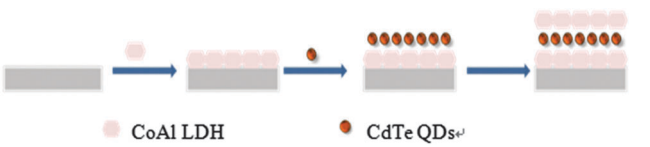

Fig. 1 Schematic representation of the LBL assembly of the $(LDH/CdTe\ QDs)_n$ multilayer films.

Mastersizer 2000 laser particle size analyzer. Fourier transform infrared (FTIR) spectra were obtained using a Vector 22 (Bruker) spectrophotometer with a resolution of 2 cm^{-1}. The morphology of the thin films was investigated using scanning electron microscopy (SEM, Hitachi S-4700) with an accelerating voltage of 20 kV. The surface roughness was studied using atomic force microscopy (AFM) software (Digital Instruments, Version 6.12). Fluorescence emission spectra were recorded on a RF-5301PC fluorophotometer (1.5 nm resolution) in the range 500–900 nm with an excitation wavelength of 480 nm and slit widths of 5 nm. A conventional three-electrode system was used, including a modified ITO glass as the working electrode, a platinum foil as the auxiliary electrode and a saturated Ag/AgCl electrode (0.799 V) as the reference electrode. The ECL signals were recorded by a MPI-B multifunctional chemiluminescence analytical system (Remax Electronic Co. Ltd, Xi'an, China) with the voltage of the photomultiplier tube (PMT) set to 800 V. The solutions were prepared with Milli-Q water (>18 MΩ cm) and purged with highly purified nitrogen. The EIS measurements were performed using a CHI 660C electrochemical workstation (Shanghai Chenhua Instrument Co.).

Sample preparation

The three different brands of sausage were pre-treated according to the following steps: 10 g of crushed sample were taken, and then 20 mL borate solution was added to turn the sausage into a paste. After that, the mixture was added to 300 mL bidistilled water at 70 °C and stirred for 20 min, and the remaining liquid was further filtered to obtain a sample stock solution.[27]

Results and discussion

Structural and morphological characterization of the $(LDH/CdTe)_n$ TFs

The scanning electron microscopy (SEM) image reveals a narrow size distribution (100–120 nm) for the individual CoAl-LDH nanoplatelets (Fig. S1A, ESI†). A clear Tyndall light scattering was observed for this well-dispersed colloidal suspension (Fig. S1B, ESI†), which was transparent and stable without any precipitation when stored under a N_2 atmosphere for more than one month. The MSA-modified CdTe QDs were synthesized *via* a hydrothermal method. The UV-vis absorption and fluorescence spectra of MSA-modified CdTe are shown in Fig. S2 (ESI†), and the CdTe solution shows strong red emission at 624 nm. In addition, high resolution transmission electron microscopy (HRTEM) shows that the MSA-modified CdTe QDs are uniform and well dispersed with a particle size of ~3.7 nm (Fig. S3, ESI†). As shown in Fig. S4 (ESI†), the zeta potential of the CdTe-QD solution is around −41 mV, which demonstrates that CdTe QDs can interact with positively charged LDH to achieve the layer-by-layer assembly. The multi-layer TFs were fabricated by alternately dipping a quartz glass slide into a colloidal LDH suspension and an aqueous solution of CdTe QDs. The fabrication process of $(LDH/CdTe\ QDs)_n$ (n = 4–20) was monitored by UV-vis absorption spectra. As shown in Fig. 2, the absorption intensity at 560 nm

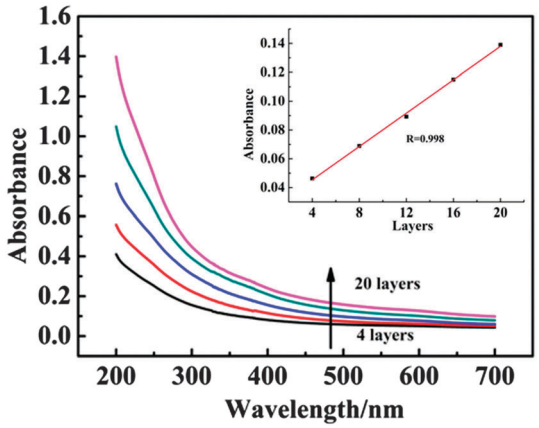

Fig. 2 UV-vis absorption spectra of the $(LDH/CdTe\ QDs)_n$ films along with the bilayer number (n = 4–20). The inset shows the absorbance intensity at 368 nm *vs.* n.

gradually increases along with the film deposition process, indicative of a stepwise and regular deposition procedure with approximately equal amounts of CdTe QDs incorporated in each cycle. In addition, the intensity of the sharp luminescence peak of the TFs with a maximum at *ca.* 624 nm also displays a monotonic increase with n (Fig. 3). The TFs under UV light irradiation (inset of Fig. 3) also reveal well-defined red luminescence with enhanced brightness upon increasing n. The fluorescence spectra of the as-prepared TFs show no obvious red or blue shift relative to that of the pristine CdTe solution, suggesting the absence of CdTe aggregates in the TFs throughout the whole assembly process. FTIR spectra of CdTe QDs, CoAl-LDH, and the $(CdTe\text{-}QDs/LDH)_{12}$ TF are shown in Fig. S5 (ESI†). After the assembly of LDH and CdTe-QDs (Fig. S5c, ESI†), the O–H absorption band around 3482 cm^{-1} and the O–M–O vibration band at 425 cm^{-1} are similar to the corresponding bands in the spectrum of the CoAl-LDH precursor. In addition, the stretching vibrations of the carboxylic groups moved to higher frequencies from 1558 to 1571 cm^{-1} and from 1372 to 1385 cm^{-1}. Such shifts may be related to host–guest interactions (such as hydrogen bonding

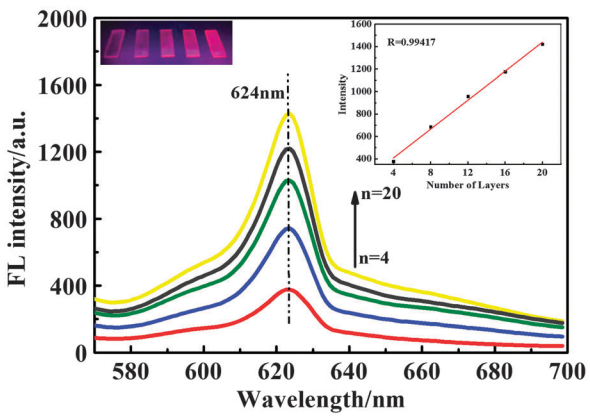

Fig. 3 Fluorescence spectra of the $(LDH/CdTe\ QDs)_n$ TFs (n = 4–20); the insets show a linear correlation between the intensity at 624 nm and n as well as the corresponding photographs under UV irradiation.

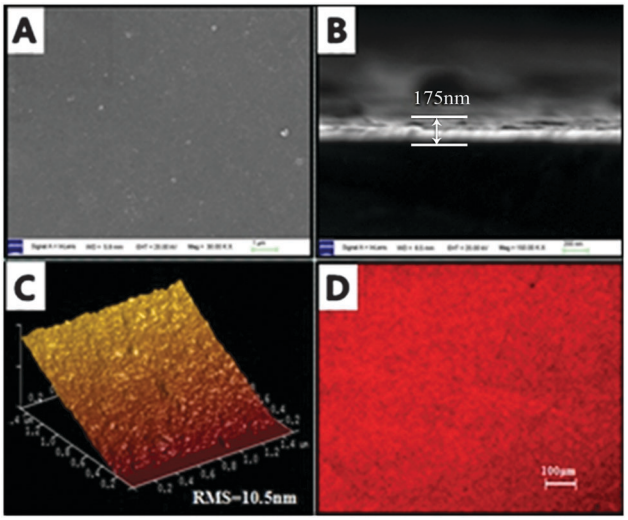

Fig. 4 Morphology of the $(LDH/CdTe\ QDs)_{12}$ TF: (A) top-view SEM image, (B) side-view SEM image, (C) tapping-mode AFM image, and (D) fluorescence microscope image.

and electrostatic forces) between the LDH layers and carboxylic acid groups in the QDs.

The surface morphology was further studied by SEM and AFM images. Taking $(LDH/CdTe\ QDs)_{12}$ as an example, the top-view SEM image (Fig. 4A) shows that the film surface is continuous and uniform; the thickness is *ca.* 175 nm as revealed by the side-view image (Fig. 4B), from which it can be estimated that the average thickness of the bilayer repeat unit is 14.9 nm. The AFM topographical image (Fig. 4C) displays a smooth surface of the film, with a root-mean-square roughness of 10.5 nm. Furthermore, the $(CdTe\ QDs/LDH)_{12}$ TF shows a homogeneous red color with strong brightness under the fluorescence microscope (Fig. 4D), indicating that the CdTe QDs are uniformly distributed throughout the TF.

Electrochemistry and ECL behavior of the sensor

Influence of the bilayer number (n) on the ECL response. The influence of the assembly number on the ECL response was first investigated. It was found that the ECL intensity of the $(LDH/CdTe\ QDs)_n$ film firstly increased upon increasing deposition cycle (n varies from 4 to 12), while a decrease in intensity was observed with further increase in n from 12 to 20 (Fig. 5). Such observation can be assigned to the fact that the CdTe concentration and impedance (Fig. S6, ESI†) of the LDH/CdTe QD-modified electrodes both increased upon increasing deposition cycle (n = 4–20), which then led to the $(LDH/CdTe)_{12}$ film with an optimal electrochemical and ECL performance. As a consequence, the film with n = 12 is chosen as the optimum electrode for ECL determination in the following section.

Enhanced anodic ECL of LDH/CdTe QDs. The anodic ECL emission of the CdTe nanoparticles in PBS was observed at a Pt disk electrode.[27] In this system, the anodic ECL emission is very weak and is not often detected even in ECL transients. However, the LDH/CdTe QDs in air-saturated PBS (pH = 7.4, detection solution) showed an intensive anodic ECL emission at the surface

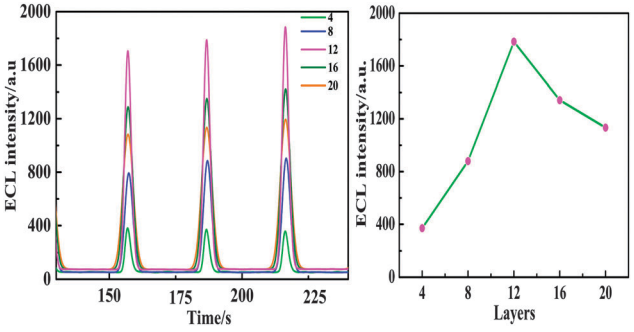

Fig. 5 ECL intensity of $(CdTe\ QDs/LDH)_n$ TFs (n = 4–20) *vs.* time (left), and the correlation between the ECL intensity and bilayer number (right), recorded in 0.18 mol L^{-1} $NaSO_3$ (pH = 7.4 in PBS, scan rate: 100 mV s^{-1}).

of the ITO electrode. Fig. 6 shows the ECL-potential curves of the CdTe QD drop-casted film, and the CdTe QDs/PDDA and CdTe QDs/LDH composite films, in both of which the quantities of the CdTe QDs are the same. Sharp ECL peaks with the same position were observed in all curves, which resulted from the reaction between the CdTe QDs and SO_3^{2-}. It was noted that the ECL intensity of the CdTe QDs/LDH composite film is about 8-fold higher than that observed for the pure CdTe QD drop-casted film. In addition, the CdTe QD drop-casted film shows a continuously decreased signal intensity (Fig. S7, ESI†). The results indicated that the existence of Co–Al-LDH nanoparticles can provide a confined microenvironment to suppress the aggregation of CdTe QDs and achieve a better conductivity of the CdTe film, thus facilitating the ECL reaction. Therefore, the as-prepared CdTe QDs/LDH TF was promising for the construction of an anodic ECL sensor.

Electrochemical impedance spectroscopy (EIS) of the sensor. EIS can offer more information about the stepwise modification and charge transfer processes. EIS is usually composed of linear and semicircle portions. The semicircle portion reflects the charge transfer resistance (R_{ct}) at high-to-medium frequencies,[28] and the linear portion represents the diffusion process at low frequencies. Herein, based on EIS, the relative R_{ct} values can be obtained for the pristine ITO, CdTe-modified ITO, LDH/CdTe and PDDA/CdTe TF electrodes, and the corresponding charge transfer

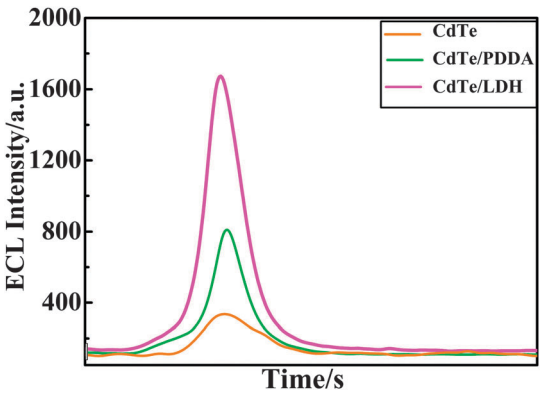

Fig. 6 ECL of drop-casted CdTe on ITO, $(PDDA/CdTe)_{12}$/ITO and $(LDH/CdTe)_{12}$/ITO recorded in 0.18 mol L^{-1} $NaSO_3$, pH = 7.4 in PBS; scan rate: 100 mV s^{-1}.

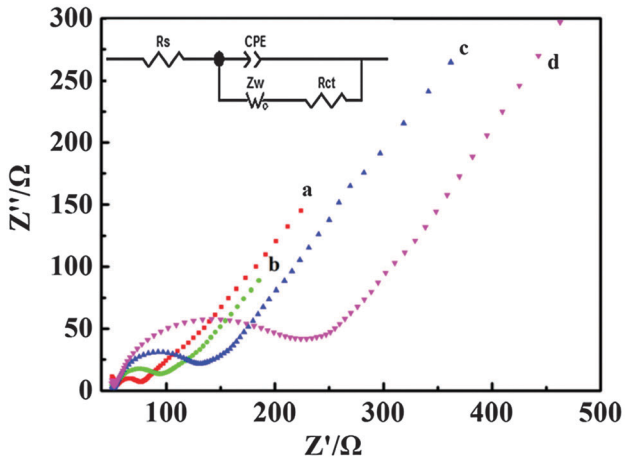

Fig. 7 Nyquist plots of EIS for (a) bare ITO, (b) CdTe/ITO, (c) $(LDH/CdTe)_{12}$/ITO and (d) $(PDDA/CdTe)_{12}$ in a 5 mM $[Fe(CN)_6]^{4-/3-}$ solution.

resistances are 79, 98, 132, and 232 Ω, respectively. Fig. 7 reveals that bare ITO exhibited a low R_{ct} (curve a) in KCl (0.1 M) containing $[Fe(CN)_6]^{3-/4-}$ (5 mM). After the bare electrode was modified with CdTe QDs, R_{ct} is highly increased (curve c) due to the low conductive properties of the CdTe units. While for the ITO electrode coated with CdTe/LDH TF (curve b), the R_{ct} showed a decreasing trend compared with that of ITO/CdTe, indicating that the CoAl-LDH nanoparticles have enhanced the electron transfer between the buffer solution and electrode surface. As a comparison, the modification with the PDDA/CdTe TF was also prepared, which led to a much larger R_{ct} (curve d) than those of both the pristine CdTe QDs and QDs/LDH TFs, due to the lack of conductive media and thus the blocking of the charge transfer. Therefore, it can be concluded that the localization of CdTe QDs onto CoAl-LDH nanoparticles can result in a highly enhanced charge transfer within the TF.

Mechanism of the anodic ECL of LDH/CdTe QDs. Based on the experimental results above and consulted literature, a possible ECL mechanism is proposed as follows. Basically, the ECL emission originates from the occurrence of electrochemical oxidization and reduction of the CdTe QDs with the co-reactant $NaSO_3$. Upon a potential scan with an initial positive direction, the CdTe QDs immobilized on the electrode were oxidized (or loss of electron) to positively charged species ($LDH/CdTe^{\bullet+}$). Meanwhile, SO_3^{2-} in solution diffused to the surface of the electrode, and could be oxidized to produce $SO_3^{\bullet-}$ species, which then reacted with dissolved oxygen to form $O_2^{\bullet-}$ radicals.[29] This is a key species to produce electron injected QDs (denoted as $LDH/CdTe^{\bullet-}$).[30] The as-formed $LDH/CdTe^{\bullet-}$ further collided with the hole-injected $LDH/CdTe^{\bullet+}$ electro-oxidization product of QDs^- to produce excited QDs*. The ECL emission occurred when QDs* returned to the ground state. Therefore, the equations corresponding to each step of the ECL mechanism are formulated as follows:

$$LDH/CdTe \rightarrow LDH/CdTe^{\bullet+} + e^-$$

$$SO_3^{2-} \rightarrow SO_3^{\bullet-} + e^-$$

$$2OH^- + SO_3^{\bullet-} + O_2 \rightarrow O_2^{\bullet-} + SO_4^{2-} + H_2O$$

$$LDH/CdTe + O_2^{\bullet-} \rightarrow LDH/CdTe^{\bullet-} + O_2$$

$$LDH/CdTe^{\bullet-} + LDH/CdTe^{\bullet+} \rightarrow LDH/CdTe + LDH/CdTe^*$$

$$LDH/CdTe^* \rightarrow LDH/CdTe + h\nu$$

ECL sensor used for temperature response. Temperature is a key factor for PL, EL and ECL processes. Although the temperature-dependent PL properties have been largely studied and developed during the last few years, how the temperature can influence the ECL is still unexplored. In this work, it was observed that the LDH/CdTe QD-modified electrode underwent a significant change in ECL intensity at different temperatures for a short period of time. The ECL peak intensity was acquired in phosphate buffer (pH = 7.4) with $NaSO_3$ as the co-reactant (Fig. 8). Upon heating the PBS and $NaSO_3$ mixed solution from 20 to 80 °C, the ECL intensity of the LDH/CdTe QD-modified electrode was gradually extenuated with a rather high response sensitivity (−1.92% per °C); moreover, the ECL intensity presents a nearly linear relationship with the temperature (Fig. 9). The decrease in ECL intensity upon increasing the temperature can be related to the fact that the heat can result in a non-radiative relaxation process, thus largely quenching the LDH/CdTe* species. In addition, the repeatability of the ECL intensity is also highly important if LDH/CdTe was to be used as a practical temperature sensor. As the solution is cooled to 20 °C, it was observed that the ECL signal could completely recover its original intensity. The

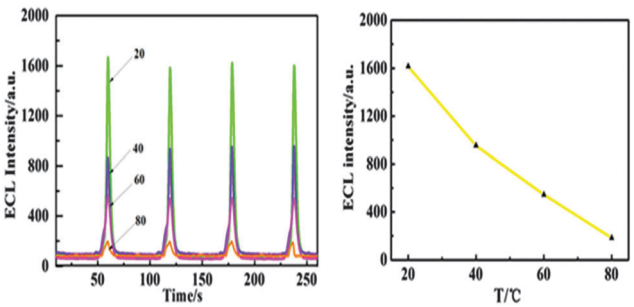

Fig. 8 ECL emission of the $(CdTe\ QDs–LDH)_{12}$ TF in the temperature range 20–80 °C (left), and the ECL intensity as a function of the temperature (right).

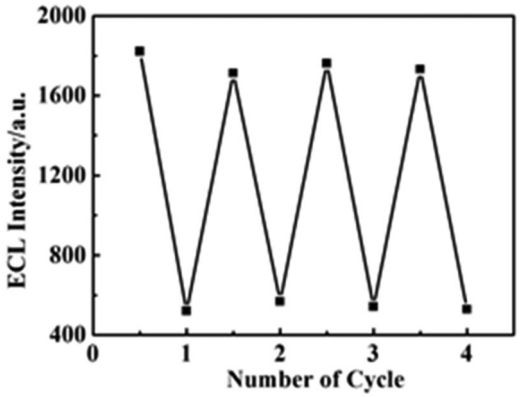

Fig. 9 Reversible variation of the ECL intensity for the $(LDH/CdTe)_{12}$ TF at 20 and 60 °C.

reversible process in the temperature range 20–60 °C can be readily repeated for at least 4 cycles. Therefore, the ECL sensor based on the LDH/CdTe TF may offer an alternative for temperature detection due to its high sensitivity and reversibility.

Nitrite detection based on the anodic ECL emission. Nitrite detection is of great importance in the environmental and public health fields. The potential transformation of nitrite into carcinogenic *N*-nitroso compounds and its widespread presence in food products and beverages have enhanced the need for its monitoring.[31–33] To date, several methods have been used to determine nitrite ions, including spectrophotometry,[34] chromatography, chemiluminescence and electrochemical methods.[35,36] However, most of them are time-consuming and require tedious sample pretreatment. Thus, the development of new sensing methods for the selective detection of nitrite is still an attractive objective. Moreover, in recent years the development of nanomaterials for the sensitive detection of nitrite has received great attention because of their unique optical, electronic, chemical and mechanical properties. Materials like chemically reduced graphene oxide,[37] gold nanoparticles,[38] metal–organic complex nanowires,[39] and QDs[40] have been applied to the detection of nitrite. Herein, it was observed that a strong anodic ECL emission of CdTe QDs could be produced, and the quenching effect of nitrite on the ECL emission *via* an "electrochemical oxidation inhibition" mechanism made it possible to detect nitrite at a relatively low potential, which largely inhibited any interference from the oxidation of other electroactive compounds. Upon addition of nitrite into the detection solution, the emission intensity of the LDH/CdTe QD-modified electrode was obviously extenuated (Fig. 10), indicating efficient ECL quenching. In our opinion, the presence of nitrite can produce a larger I_R drop which makes the practical potential E_w less than the applied potential E:[41] $E_w = E - I_R = E - (I_q + I_{emitter})R$, where I_q and $I_{emitter}$ are the oxidation currents of the quencher and light-emitter. The lower E_w decreases the oxidation of the light-emitter, leading to a weaker ECL emission. Based on the quenching effect on the anodic ECL emission of CdTe QDs, a rapid detection method for nitrite could be developed. The ratio of the initial ECL intensity I_0 to the intensity I with nitrite concentrations ranging from 1 μM to 0.01 M showed a linear relation (R = 0.996).

The limit of detection (LOD) can be further determined as 0.719 μM. The relative standard deviation (RSD) was calculated as 3.7% for six successive detections at 5 μmol L^{-1}. Compared with the as-reported systems for the detection of nitrite (Table S1, ESI†),[42–48] the proposed method exhibits a wider linear range and a comparable limit of detection, indicating that the QD-based sensor presents a high detection performance. Furthermore, the prepared electrode showed a good analytical performance in terms of being low-cost, reliable, effortless and fast.

Specificity, repeatability and stability of the sensor. To evaluate the selectivity and specificity of the present sensor, several similar inorganic and organic species (such as K^+, Na^+, Mg^{2+}, CO_3^{2-}, SO_4^{2-}, Cl^-, NO_3^-, glucose, and citric acid) were also tested under the same conditions as in the case of NO_2^-. As shown in Fig. 11, there is only a slight decrease in ECL intensity for these anions, and their quenching effects were not as obvious as that of NO_2^-, indicating a high ECL selectivity of the CdTe/LDH sensor for NO_2^-.

The reproducibility of the sensor was estimated by determining the regeneration of the ECL signal of the LDH/CdTe film. After four cycles by alternate treatment with 0.01 M nitrite and PBS, the sensor still presents strong ECL and maintains nearly the same intensity,

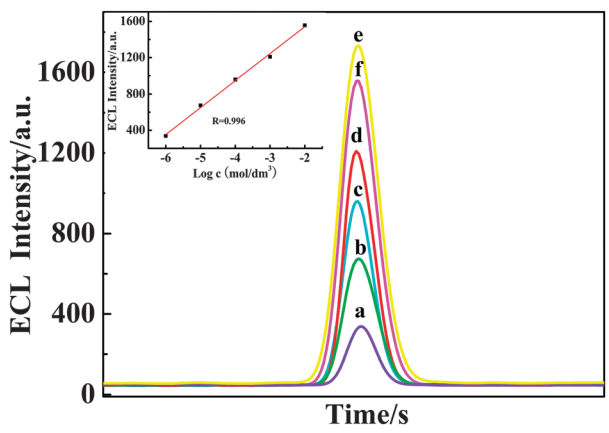

Fig. 10 ECL intensity of the $(LDH/CdTe)_{12}$ modified electrode in 0.1 M PBS (pH = 7.4) in the presence of $NaNO_2$ with various concentrations (from e to b: 1×10^{-6} to 1×10^{-2} M). Scan rate: 100 mV s^{-1}. The inset shows the plot of ECL intensity *vs.* $NaNO_2$ concentration.

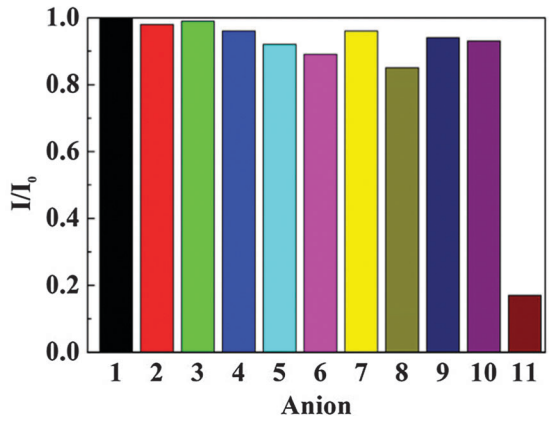

Fig. 11 Change of the ECL intensity, normalized to a blank, after being challenged with interfering anions: (1) blank, (2) K^+, (3) Na^+, (4) Mg^{2+}, (5) CO_3^{2-}, (6) SO_4^{2-}, (7) Cl^-, (8) NO_3^-, (9) glucose, (10) citric acid, and (11) NO_2^-.

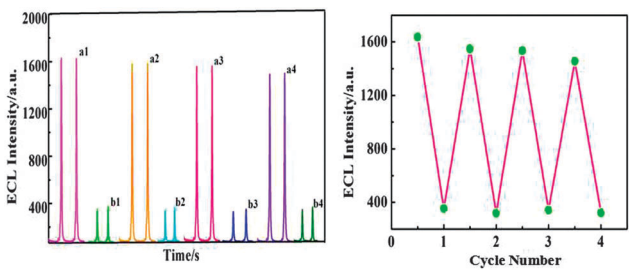

Fig. 12 ECL signal quenching and recovery cycles for the $(CdTe/LDH)_{12}$-modified ITO electrode after alternate treatments by PBS and 0.01 M $NaNO_2$ solutions (left), and the ECL intensities over four continuous cycles (right).

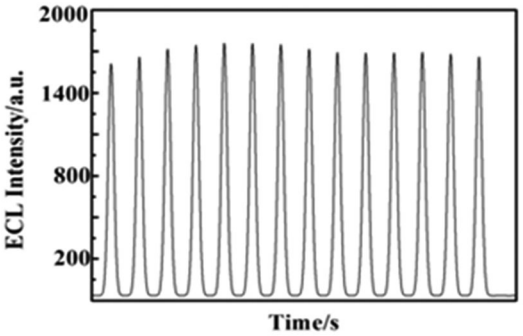

Fig. 13 ECL emission of the $(LDH/CdTe)_{12}$-modified ITO electrode in 0.1 M PBS (pH = 7.4) under continuous Cyclic Voltammetry (CV) for 14 cycles. Scan rate: 100 mV s^{-1}.

Table 1 Determination of nitrite in sausage samples

Sample	ECL method[a] (NO_2^-, μmol L^{-1})	Spectroscopy (NO_2^-, μmol L^{-1})	Added[a] (NO_2^-, μmol L^{-1})	Found[a] (NO_2^-, μmol L^{-1})	Recovery (%)
1	3.12 ± 0.13	3.20	2	5.18 ± 0.21	106.5
2	2.67 ± 0.10	2.58	2	4.70 ± 0.12	101.5
3	2.82 ± 0.20	2.71	2	4.75 ± 0.15	96.5

[a] Mean ± SD of three measurements.

confirming the reusability of the sensor (Fig. 12). Therefore, the $(LDH/CdTe)_{12}$ ECL sensor is feasible and can be used for the determination of nitrite. Furthermore, a study was carried out to illustrate the stability of the modified electrode. After dipping the modified electrode into PBS (pH = 7.4) for 10 days, the $(CdTe/LDH)_{12}$-modified electrode still exhibited good stability under continuous potential scanning for 14 cycles (as shown in Fig. 13, RSD = 6%). No obvious decline in intensity was observed for the solid-state ECL TF, demonstrating that the sensor shows good stability.

Real sample detection. To examine the potential of the proposed method in a practical application, experiments were further performed on samples of a real sausage (three different brands) for the determination of possible nitrite. As shown in Table 1, the results are comparable with those obtained by a spectroscopic method for the sample determination. Moreover, recovery studies were also carried out on the samples by adding extra standard nitrite. It can be seen that the recoveries were in the range of 96–107%, suggesting that the method has high accuracy. Thus the proposed method provides an effective alternative for the determination of nitrite in real samples.

Conclusion

In summary, in this work we developed a bi-functionalized QD-based ECL sensor for the response to temperature and the detection of nitrite. ECL emitter QDs were successfully fabricated on ITO electrodes *via* LBL assembly with Co–Al-LDH nanoparticles. UV-visible and fluorescence spectra confirm a stepwise and regular assembly process of the TFs. The structural and morphological studies show that the film surface is continuous and uniform with long range stacking order in the normal direction of the substrate. The electrochemical and ECL behaviors of the CdTe/LDH film modified electrodes were studied in detail. Comparison studies demonstrate that the LDH/CdTe TF displays improved electron transfer and ECL efficiency. The modified electrode exhibited significant and reversible transformation of the emissive intensity in the temperature range 20–80 °C. Moreover, LDH/CdTe exhibits a sensitive response for nitrite with high selectivity, acceptable storage stability, good precision and repeatability. Therefore, this work provides a facile approach to enhanced QD ECL based on a long-range order architecture comprising CdTe QDs and LDH nanoparticles, which could open up an effective way to apply QDs in anodic ECL sensor systems.

Acknowledgements

This work was supported by the National Natural Science Foundation of China (NSFC), National Basic Research Program of China (973 Program) (Grant No. 2014CB932103), and Beijing Municipal Natural Science Foundation (Grant No. 2152016).

Notes and references

1 M. M. Richter, *Chem. Rev.*, 2004, **104**, 3003.
2 A. W. Knight, *TrAC, Trends Anal. Chem.*, 1999, **18**, 47.
3 Z. Ding, B. M. Quinn, S. K. Haram, L. E. Pell, B. A. Korgel and A. J. Bard, *Science*, 2002, **296**, 1293.
4 Y. Yu, M. Zhou and H. Cui, *J. Mater. Chem.*, 2011, **21**, 12622.
5 S. Ding, J. Xu and H. Chen, *Chem. Commun.*, 2006, 3631.
6 H. Jiang and H. Ju, *Anal. Chem.*, 2007, **79**, 6690.
7 H. Dhyani, M. A. Ali, M. K. Pandey and P. Sen, *J. Mater. Chem.*, 2012, **20**, 4970.
8 H. Jiang and H. Ju, *Chem. Commun.*, 2007, 404.
9 W. Miao, *Chem. Rev.*, 2008, **108**, 2506.
10 L. Dennany, M. Gerlach, S. O'Carrol, T. E. Keys, R. J. Forster and P. Bertoncello, *J. Mater. Chem.*, 2011, **21**, 13984.
11 X. Liu and H. Ju, *Anal. Chem.*, 2008, **80**, 5377.
12 G. J. Barbante, C. F. Hogan, A. Mechler and A. B. Hughes, *J. Mater. Chem.*, 2010, **20**, 891.
13 D. Yuan, S. Chen, R. Yuan, J. Zhang and X. Liu, *Sens. Actuators, B*, 2014, **191**, 415.
14 (*a*) H. Niu, R. Yuan, Y. Chai, L. Mao, H. Liu and Y. Cao, *Biosens. Bioelectron.*, 2013, **39**, 296; (*b*) G. Jie, J. Yuan and J. Zhang, *Biosens. Bioelectron.*, 2012, **31**, 69; (*c*) G. Jie, L. Wang and S. Zhang, *Chem. – Eur. J.*, 2011, **17**, 641.
15 G. Jie, B. Liu, H. Pan, J. Zhu and H. Chen, *Anal. Chem.*, 2007, **79**, 5574.
16 M. Yan, W. Gao, S. Ge, L. Ge, C. Chu, J. Yu and S. Hou, *J. Mater. Chem.*, 2012, **22**, 5568.
17 G. Jie and J. Yuan, *Anal. Chem.*, 2012, **84**, 2811.
18 G. R. Williams and D. O'Hare, *J. Mater. Chem.*, 2006, **26**, 3065.
19 (*a*) D. P. Yan, J. Lu, M. Wei, D. G. Evans and X. Duan, *J. Mater. Chem.*, 2011, **21**, 13128; (*b*) H. Y. Ma, R. Gao, D. P. Yan, J. W. Zhao and M. Wei, *J. Mater. Chem. C*, 2013, **1**, 4128;

(*c*) D. P. Yan, J. Lu, J. Ma, M. Wei, S. H. Qin, L. Chen, D. G. Evans and X. Duan, *J. Mater. Chem.*, 2010, **20**, 5016.
20 J. Han, X. Xu, X. Rao, M. Wei, D. G. Evans and X. Duan, *J. Mater. Chem.*, 2011, **21**, 2126.
21 E. Scavetta, M. Berrettoni, F. Nobili and D. Tonelli, *Electrochim. Acta*, 2005, **50**, 3305.
22 D. Shan, S. Cosnier and C. Mousty, *Anal. Chem.*, 2003, **75**, 3872.
23 R. Tian, R. Liang, D. Yan, W. Shi, X. Yu, M. Wei, L. S. Li, D. G. Evans and X. Duan, *J. Mater. Chem.*, 2013, **1**, 5654.
24 R. Liang, D. Yan, R. Tian, X. Yu, W. Shi, C. Li, M. Wei, D. G. Evans and X. Duan, *Chem. Mater.*, 2014, **26**, 2595.
25 N. Gaponik, D. V. Talapin, A. L. Rogach, K. Hoppe, E. V. Shevchenko, A. Kornowski, A. Eychmuller and H. Weller, *J. Phys. Chem. B*, 2002, **106**, 7177.
26 Y. Zhao, F. Li, R. Zhang, D. G. Evans and X. Duan, *Chem. Mater.*, 2002, **14**, 4286.
27 A. Akhami, T. Madrakian and H. Ghaedi, *Electrochim. Acta*, 2012, **66**, 25.
28 Y. Bae, N. Myung and A. J. Bard, *Nano Lett.*, 2004, **4**, 1153.
29 B. Ballarin, M. C. Cassani, E. Scavetta and D. Tonelli, *Electrochim. Acta*, 2008, **53**, 8034.
30 X. Liu and H. Ju, *Anal. Chem.*, 2008, **80**, 5377.
31 S. K. Poznyak, D. V. Talapin, E. V. Shevchenko and H. Weller, *Nano Lett.*, 2004, **4**, 693.
32 F. Liao, X. Song, S. Yang, C. Hu, L. He and G. Ding, *J. Mater. Chem. A*, 2015, **3**, 7568.
33 I. M. P. L. V. O. Ferreira and S. Silva, *Talanta*, 2008, **74**, 1598.
34 K. Thenmozhi and S. S. Narayanan, *Electroanalysis*, 2007, **19**, 2362.
35 X. Liu, L. Guo, L. Cheng and H. Ju, *Talanta*, 2009, **78**, 691.
36 G. Bharath, R. Madhu, S. Chen, V. Veeramani and N. Ponpandian, *J. Mater. Chem. A*, 2013, 1.
37 V. Mani, A. P. Periasamy and S. Chen, *Electrochem. Commun.*, 2012, **17**, 75.
38 W. L. Daniel, M. S. Han and J. Lee, *J. Am. Chem. Soc.*, 2009, **131**, 6362.
39 Q. Li, J. Zheng and Y. Yan, *Adv. Mater.*, 2012, **19**, 31.
40 L. Liu, Q. Ma, Z. Liu and Y. Li, *Anal. Bioanal. Chem.*, 2014, **406**, 879.
41 P. K. Rastogi, V. Ganesan and S. Krishnamoorthi, *J. Mater. Chem. A*, 2014, **2**, 933.
42 F. Kuralay, M. Dumangöz and S. Tunc, *Talanta*, 2015, **144**, 1133.
43 H. Liu, G. Yang and J. Zhu, *Talanta*, 2013, **104**, 135.
44 J. Li, Q. Li, C. Lu and L. Zhao, *Analyst*, 2011, **136**, 2379.
45 X. Huang, Y. Li, Y. Chen and L. Wang, *Sens. Actuators, B*, 2008, **134**, 780.
46 Z. Lin, W. Xue, H. Chen and J. Lin, *Anal. Chem.*, 2011, **83**, 8245.
47 L. Monser, S. Sadok, G. Greenway, I. Shah and R. Uglow, *Talanta*, 2002, **57**, 511.
48 K. Kwan, K. L. Kyung and S. S. Kuan, *Analyst*, 2012, **137**, 3836.

